

# Monte Carlo Investigation of Traveling Accumulation Layers in InP Heterojunction Bipolar Transistor Power Amplifiers

Jonathan P. Sculley  
Georgia Institute of Technology  
Atlanta, USA  
[jonathan.sculley@gatech.edu](mailto:jonathan.sculley@gatech.edu)

Brian Markman  
University of California  
Santa Barbara, USA  
[brianmarkman@ucsb.edu](mailto:brianmarkman@ucsb.edu)

Utku Soyulu  
University of California  
Santa Barbara, USA  
[utkusoyulu@ucsb.edu](mailto:utkusoyulu@ucsb.edu)

Yihao Fang  
University of California  
Santa Barbara, USA  
[yihao.fang@ucsb.edu](mailto:yihao.fang@ucsb.edu)

Miguel E. Urteaga  
Teledyne Scientific and Imaging  
Thousand Oaks, USA  
[miguel.urteaga@teledyne.com](mailto:miguel.urteaga@teledyne.com)

Andy D. Carter  
Teledyne Scientific and Imaging  
Thousand Oaks, USA  
[andy.carter@teledyne.com](mailto:andy.carter@teledyne.com)

Mark J. W. Rodwell  
University of California  
Santa Barbara, USA  
[rodwell@ucsb.edu](mailto:rodwell@ucsb.edu)

Paul D. Yoder  
Georgia Institute of Technology  
Atlanta, USA  
[doug.yoder@gatech.edu](mailto:doug.yoder@gatech.edu)

**Abstract**— We report Monte Carlo simulation results of 300nm InP heterojunction bipolar transistors driven to exhibit distortion. IM3 distortion is typically explained by collector velocity modulation. Full-band ensemble Monte Carlo simulations implicate intervalley transfer as an additional source of distortion under conditions of high current, low voltage, and high doping. Simulations reveal that intervalley transfer promotes the formation of traveling accumulation domains which result in high frequency distortion more significant than that caused by velocity modulation. Special care must be taken when designing high current HBT power amplifiers in order to mitigate this effect.

**Keywords**—InP HBT, velocity modulation, transit-time modulation, Gunn effect, transferred electron effect, Monte Carlo simulation, IM3 distortion

## I. INTRODUCTION

InP heterojunction bipolar transistors (HBTs) are useful for high efficiency wideband medium-power amplifiers from 30-300 GHz. One of the primary concerns for these power amplifiers is 3<sup>rd</sup> order intermodulation distortion (IM3) [1-2]. Collector velocity modulation is well known to cause significant IM3. Collector velocity modulation models are built into modern HBT computer-aided design (CAD) software such as Keysight's Advanced Design System. These models reveal that collector velocity modulation is often the primary contributor to IM3 distortion in well-designed HBT power amplifiers. The analysis by Betser [1] is quasi-static and thus cannot account for charge domain instabilities. The analysis by Urteaga [2] takes second-order temporal dynamics into consideration (correct to order  $\omega^2 \tau_c^2$ ), but it too does not incorporate the physics required to describe traveling charge domains.

We here report detailed Monte Carlo simulations of electron transport in InP HBTs. In addition to collector velocity modulation, and strongly related to it, under the conditions of high current, low voltage, and high doping, the nucleation, growth and propagation of traveling charge domains [3-5] in the collector is observed. The resulting effects can produce

distortion in the collector current waveforms well beyond that predicted by quasi-static electron velocity modulation models; therefore, this effect must be considered in HBT design. The presence of this effect may significantly change the high-frequency 2-port parameters at frequencies close to that of the inverse of the carrier transit time, so circuits must be designed appropriately.

Traveling charge domains in materials with negative differential resistance (NDR) typically consist of an electron accumulation layer upstream from an electron depletion layer. This dipole increases the electric field seen by the accumulated electrons which decreases their velocity if the biasing electric field is in the NDR regime. Faster upstream electrons join the accumulation layer and faster downstream electrons move farther away thereby growing both the accumulation and depletion layers while propagating. Traveling accumulation layers are less common and behave similarly to traveling dipole domains, and they consist of only an electron accumulation without a depletion layer.

Traveling charge domains due to the transferred electron effect have previously been predicted through hydrodynamic simulation [6-7] and experimentally demonstrated in GaAs HBTs [8]. Previous simulation work using hydrodynamic models suffer from several limitations when compared to Monte Carlo simulation. While hydrodynamic simulations are able to demonstrate negative differential resistance, the hydrodynamic model itself does not correctly account for the energy and valley dependence of energy and momentum relaxation, which are fundamental to the phenomenon of intervalley transfer. Indeed, hydrodynamic and energy balance models are notorious for their predictions of anomalous velocity overshoot in ultra-scaled metal-oxide-semiconductor field-effect-transistors (MOSFETs) [9-11]. Monte Carlo simulations utilizing a 3-valley band model have confirmed the formation of traveling charge domains in a GaAs heterojunction bipolar transferred electron device (HBTED) [12], but the authors are not aware of any Monte Carlo investigations of this effect in InP devices, or of any Monte

Carlo simulations which utilize a full band structure to study this effect in any material system. While it has been suggested that the Gunn effect can only occur at current levels above the Kirk threshold [13], the inclusion of a delta doped layer can raise the Kirk threshold sufficiently to observe the formation of charge domain instabilities before the onset of base pushout.

## II. SIMULATION MODEL

In this work, we use a full-band ensemble Monte Carlo device simulator to model carrier transport within the base and collector regions of an InP double HBT (DHBT). The electron and hole dispersion relations were calculated using the empirical pseudopotential method. The simulated scattering mechanisms include polar optical phonon scattering, acoustic phonon scattering, ionized impurity scattering, carrier-carrier scattering, and impact ionization [14-15].

The Monte Carlo method accounts rigorously for the physics of semiclassical charge transport, enabling predictive modeling of dynamic differential mobility and other complex effects which occur during device operation. In particular, the Monte Carlo method has demonstrated that even in bulk material, the transient velocity-field relationship can differ substantially from the static velocity-field relationship on time scales approaching the energy and momentum relaxation times [14, 16] This is especially important at high frequencies where electron velocity is far from the steady state value.

Simulations were performed on the base-collector region of a 300 nm InP DHBT with layer structure shown in Table 1.

TABLE I. SIMULATED LAYER STRUCTURE

Layer Name	Material	Thickness [nm]	Doping [ $\text{cm}^{-3}$ ]
Base	InGaAs	40	$6 \times 10^{19}$
Setback	InGaAs	5	$10^{16}$
Grade	InGaAsP	16.5	$10^{16}$
Delta	InP	3	$3.5 \times 10^{18}$
Collector	InP	275.5	$10^{16}$ to $4 \times 10^{16}$
Sub-collector	InP	3000	$2 \times 10^{19}$

The device is simulated in a common-base configuration shown in Fig. 1 with a load resistance,  $R_L$ , between the collector and the DC voltage source,  $V_{cc}$ . Instantaneous collector current is calculated according to the Ramo-Shockley theorem [17]

considering contributions from both carrier motion and displacement current. The device is stimulated by both DC and large-signal RF electron injection current,  $J_{n,e}$ , at the emitter side of the quasi-neutral base.

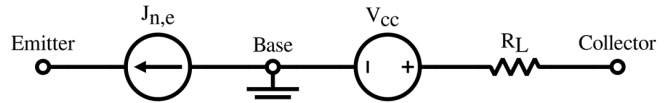


Fig 1. Terminal biasing used in all simulations.  $J_{n,e}$  is the stimulating DC or RF electron current injected into the base,  $V_{cc}$  is the DC source voltage, and  $R_L$  is the load resistance.

## III. SIMULATION RESULTS

For all reported simulations, the source voltage was fixed at 17 V and the load resistance was set to  $6.6 \text{ k}\Omega\text{-}\mu\text{m}^2$ . Simulations were performed for both DC and RF injected electron current. The simulated RF condition consisted of a 30 GHz sinusoidal current varying between 0 and  $2 \text{ mA}/\mu\text{m}^2$ . The simulated DC condition was a fixed  $2 \text{ mA}/\mu\text{m}^2$  electron current.

As the DC simulation is continuously within the high current, low voltage regime, electron accumulation layers continuously form near the base and grow while propagating through the collector until impinging upon the sub-collector. This carrier motion results in collector current oscillations as shown in Fig. 2 (a). Under RF stimulation, accumulation layers do not form during the majority of each period as electron density is too low. However, when collector current is near its maximum value, the electron density is large enough to sustain a traveling accumulation layer. Under these conditions, two accumulation layers successively propagate during each period with the resulting collector current shown in Fig. 2 (b).

Under both DC and RF conditions, the accumulation layers reach a much smaller size when the collector doping is at its lowest value of  $10^{16}/\text{cm}^3$ . Under RF stimulation, the collector current distortion observed is primarily caused by velocity modulation for low collector doping densities. Under low collector-base voltage,  $V_{cb}$ , conditions, band bending reduces field strengths near the base and thus increases the distance required for electrons to travel in order to gain enough energy to scatter into satellite valleys. This results in a dead zone where

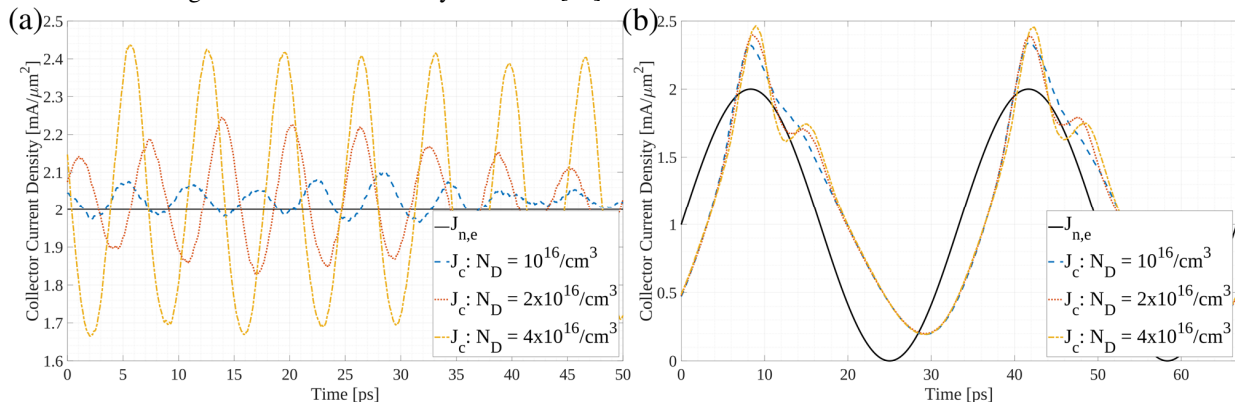


Fig 2. Collector current versus time for a DC injected current (a) and an RF injected current (b). For DC, electron accumulation domains continuously form, grow, and propagate towards the sub-collector resulting in collector current oscillations. Under an RF injected current, accumulation domains are only able to grow and propagate near the peak current. During each period, two successive accumulation domains form and propagate, resulting in the current waveform's double peak. At the lowest doping level,  $10^{16}/\text{cm}^3$ , the accumulation layers are small and the distortion of the RF waveform is primarily due to velocity modulation.

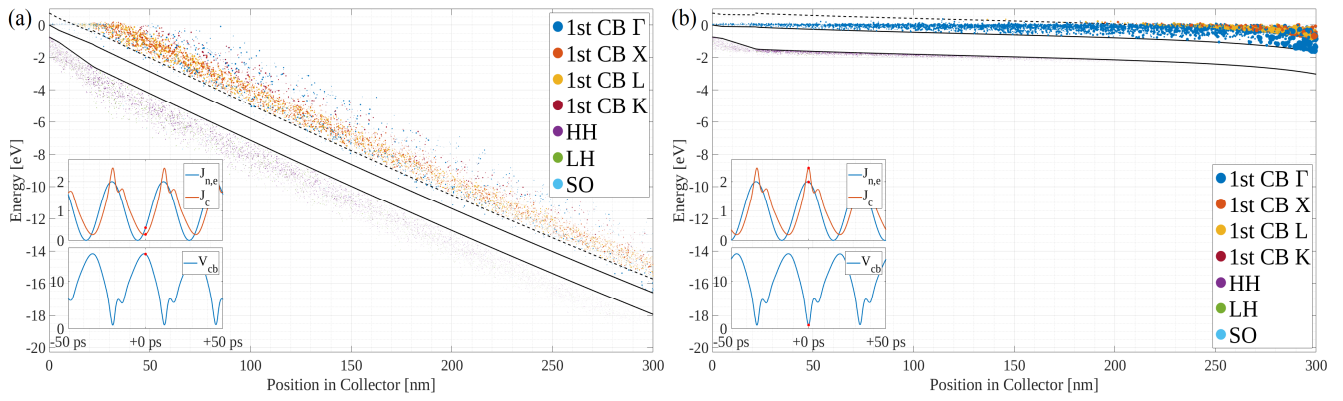


Fig 3. Band diagram and carrier energy distributions at two points in time for an RF simulation with  $N_D = 4 \times 10^{16} / \text{cm}^3$ : minimum current, maximum voltage (a) and maximum current, minimum voltage (b). In both plots the dotted line above the conduction band represents the L-valley minimum energy. In the first case, there is almost no band bending due to the low current and the electric field is also large, so electrons gain enough energy to scatter into the satellite valleys over a very short distance. In the second case, the electric field is very weak throughout the majority of the collector due to a combination of the small potential and the severe band bending.

traveling accumulation layers cannot exist. This dead zone can be observed in Fig. 3 as its minimum when  $V_{cb}$  is large (a) and its maximum when  $V_{cb}$  is small (b). Accumulation layers typically start to form approximately halfway into the collector under low doping conditions. At higher doping levels, band bending is reduced and the electric field is increased near the base, so electrons gain enough energy to reach the satellite

valleys over a shorter distance, reducing the size of the dead zone and encouraging traveling accumulation layer formation nearer the base. The dynamics of both the electron density and the electric field strength are illustrated in Fig. 4 for both DC and RF injection current. Under both conditions, electrons begin to accumulate shortly after the dead zone.

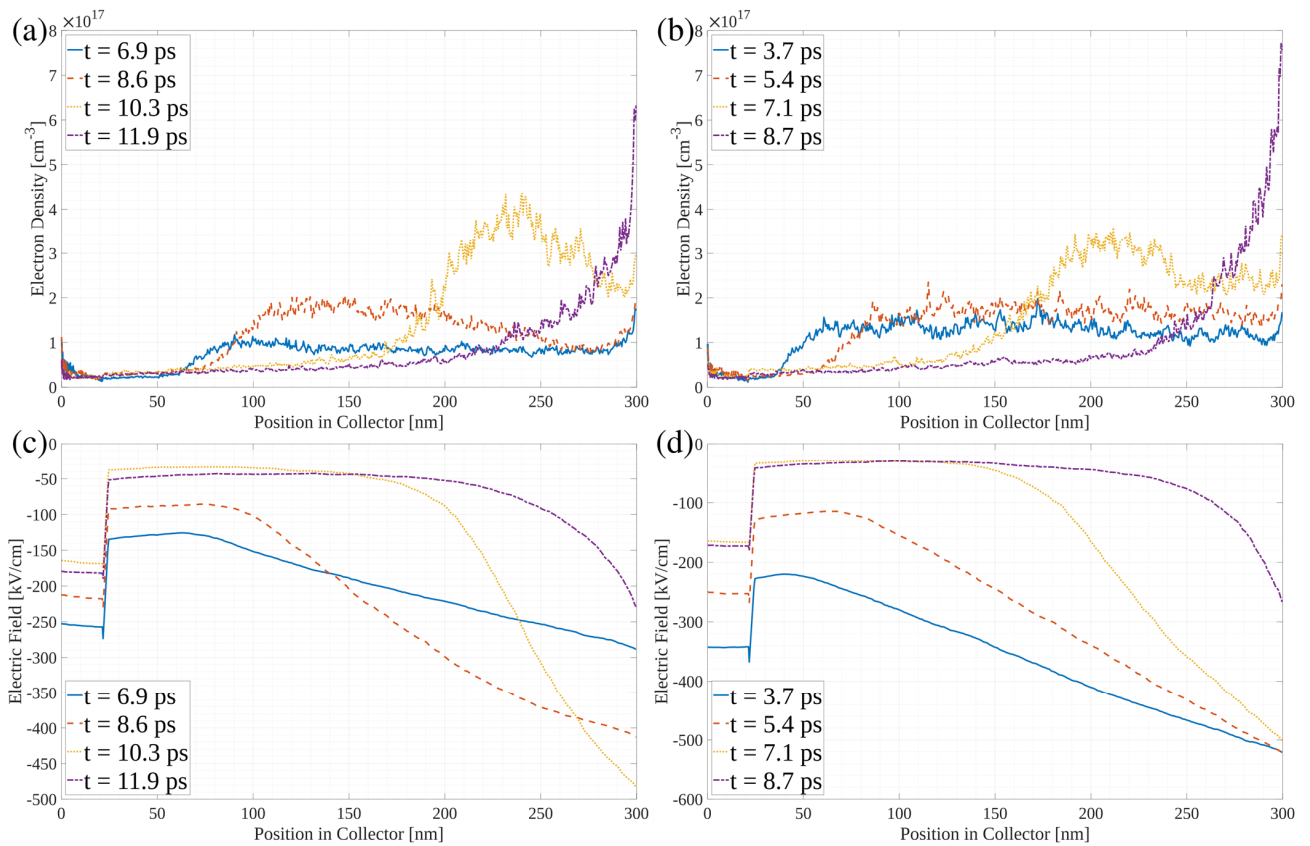


Fig 4. Time evolution of the electron density for DC (a) and RF (b) and electric field for DC (c) and RF (d) throughout the life of a traveling accumulation layer with  $4 \times 10^{16} / \text{cm}^3$  collector doping. The electron accumulation layer initially forms close to the base. It then propagates while growing and impinges upon the sub-collector after 5 ps.

#### IV. CONCLUSION

Through Monte Carlo simulation the formation of traveling charge domain instabilities has been shown to occur in InP DHBTs at current levels below the onset of the Kirk effect. Charge domain instabilities can result in significant distortion of the collector current under conditions of high current, low voltage, and high collector doping. The charge domain instability appears as a pure accumulation domain rather than the more familiar dipole domain because it nucleates, grows and propagates in an already fully depleted collector layer. As a result of this effect, special care must be taken, especially at frequencies near the reciprocal of the electron transit time, as it could severely affect 2-port parameters in a way not predicted by current state of the art design tools.

#### REFERENCES

- [1] Y. Betsler and D. Ritter, "Reduction of the base-collector capacitance in InP/GaInAs heterojunction bipolar transistors due to electron velocity modulation," *IEEE Transactions On Electron Devices*, vol. 46, pp. 628-633, April 1999
- [2] M. Urteaga, M. J. W. Rodwell, "Power gain singularities in transferred-substrate InAlAs/InGaAs HBT's," *IEEE Transactions on Electron Devices*, vol. 50, July 2003
- [3] J. B. Gunn, "Instabilities of current in III-V semiconductors," *IBM Journal of Research and Development*, vol. 8, pp. 141-159, April 1964
- [4] B. K. Ridley, "Specific negative resistance in solids," *Proceedings of the Physical Society*, vol. 82, pp. 954-954, December 1963
- [5] H. Kroemmer, "Theory of the Gunn effect," *Proceedings of the IEEE*, vol. 52, pp. 1736-1736, December 1964
- [6] V. A. Posse and B. Jalali, "Gunn effect in heterojunction bipolar transistors," *Electronics Letters*, vol. 30, pp. 1183-1184, July 1994
- [7] V. A. Posse and B. Jalali, "Transferred-electron induced current instabilities in heterojunction bipolar transistors," *Applied Physics Letters*, vol. 66, pp. 3319-3321, June 1995
- [8] J. K. Twynam, M. Yagura, N. Takahashi, E. Suematsu, and H. Sato, "Demonstration of a 77-GHz heterojunction bipolar transferred electron device," *IEEE Electron Device Letters*, vol. 21, pp. 2-4, January 2000
- [9] T. Grasser, T. W. Tang, H. Kosina, and S. Selberherr, "A review of hydrodynamic and energy-transport models for semiconductor device simulation," *Proceedings of the IEEE*, vol. 91, pp. 251-274, April 2003
- [10] D. Munteanua and G. Le Carval, "Assessment of Anomalous Behavior in Hydrodynamic Simulation of CMOS Bulk and Partially Depleted SOI Devices," *Journal of The Electrochemical Society*, vol. 149, pp. 574-580, October 2002
- [11] K. Souissi, F. Odeh, H. H. K. Tang, and A. Gnudi, "Comparative Studies of Hydrodynamic and Energy Transport Models," *The international journal for computation and mathematics in electrical and electronic engineering*, vol. 13, pp. 439-453, February 1994
- [12] J. K. Twynam, et al., "Design and analysis of heterojunction bipolar transferred electron devices," *IEEE Transactions on Electron Devices*, vol. 48, pp. 1531-1539, August 2001
- [13] M. Rudolph, R. Doerner, and P. Heymann, "On the Gunn effect in GaAs HBTs," *IEEE MTT-S International Microwave Symposium Digest*, vol. 2, pp. 683-686, May 2001
- [14] S. Sridharan and P. D. Yoder, "Anisotropic transient and stationary electron velocity in bulk wurtzite GaN," *IEEE Electron Device Letters*, vol. 29, pp. 1190-1192, November 2008
- [15] S. Sridharan, A. Christensen, A. Venkatachalam, S. Graham, and P. D. Yoder, "Temperature- and Doping-Dependent Anisotropic Stationary Electron Velocity in Wurtzite GaN," *IEEE Electron Device Letters*, vol. 32, pp. 1522-1524, September 2011
- [16] T. J. Maloney and J. Frey, "Transient and steady-state electron transport properties of GaAs and InP," *Journal of Applied Physics*, vol. 48, pp. 781-787, February 1977
- [17] P. D. Yoder, K. Gärtner, and W. Fichtner, "A generalized Ramo-Shockley theorem for classical to quantum transport at arbitrary frequencies," *Journal of Applied Physics*, vol. 79, pp. 1951-1954, February 1996